CONCEPT OF A BATTERY AGING MODEL FOR LITHIUM-ION BATTERIES CONSIDERING THE LIFETIME DEPENDENCY ON THE OPERATION STRATEGY

Conference Paper · September 2009

DOI: 10.4229/24thEUPVSEC2009-4BO.11.3

Dirk Magnor
RWTH Aachen University

Jochen Bernhard Gerschler
BMW Group

Dirk Uwe Sauer
RWTH Aachen University

CONCEPT OF A BATTERY AGING MODEL FOR LITHIUM-ION BATTERIES CONSIDERING THE LIFETIME DEPENDENCY ON THE OPERATION STRATEGY

Dirk Magnor[1], Jochen Bernhard Gerschler[1], Madeleine Ecker[1], Peter Merk[1], Dirk Uwe Sauer[1]

Electrochemical Energy Conversion and Storage Systems Group
Institute for Power Electronics and Electrical Drives, RWTH Aachen University
Jaegerstrasse 17/19, 52066 Aachen, Germany
Tel.: +49 241 80 96981, Fax: +49 241 80 92203
E-Mail: ma@isea.rwth-aachen.de

ABSTRACT: Especially in applications with long system lifetimes like PV systems or electro-mobility applications, the battery share of the overall systems' life cycle cost (LCC) is significant, due to the relatively high investment cost and the limited lifetimes of most battery systems. The battery lifetimes on the other hand are depending on a variety of parameters, some of which can be influenced by the operation strategy. In order to optimize the life cycle cost of the system two main questions have to be answered regarding the battery: what is the optimum battery size and how to control the operation strategy of the system. This paper shows a modeling approach that takes into consideration the battery lifetime depending on operation parameters like state of charge (SOC) or in fact the potential and the depth of the cycles ΔSOC. The presented model approach offers the chance of predicting the battery lifetime depending on the operation conditions of a given application more precisely. This paves the way for an optimization of the energy and also the battery management system in order to minimize the LCC of the overall system.

1 INTRODUCTION

Life cycle cost assessment is an important tool in order to optimize a system with respect to its total cost over the system lifetime. Though the significance of the life cycle cost assessment is limited by the accuracy of the assumptions made. As the aging behavior of batteries is a very complex issue, even small changes in operation parameters can change the batteries' lifetime and therefore influence its life cycle cost. To be able to predict the behavior of the battery with respect to the expected operation conditions it is necessary to account for the different impact factors on battery aging like the cycle depth, the battery potential, the temperature and the superposition of macro and micro cycles. The model presented in this paper takes under consideration these different impact factors and calculates the resulting "consumption of lifetime" on a heuristic base.

2 BATTERY AGING

The aging of batteries is very complex due to the complexity of its electrochemical nature. When talking about aging, it is important to differentiate between aging effects, aging mechanisms and impact factors.

Aging Effects: The aging effects describe the change in battery behavior at the terminals thus are important for the operator and have to be considered during battery design for a given application. The most obvious aging effects are the decrease of capacity and the increase of the internal resistance. For most applications the end of life (EOL) of a battery is determined by the minimum allowed remaining capacity and the maximum allowed internal resistance and therefore depends on the aging effects.

Impact Factors on Aging: The impact factors are environmental and operation parameters influencing the aging of a battery. In terms of modeling they can be thought of as the input parameters. Well known is the influence of the potential, the temperature and the cycle depth ΔSOC of a cycle.

Aging Mechanisms: The physico-chemical processes taking place inside the battery, causing the aging effects to appear are called aging mechanisms. The aging mechanisms are influenced by the impact factors and are causing the aging effects to occur. A summary of aging mechanisms in lithium-ion batteries is given in [3]. Some examples for aging mechanisms are corrosion, loss of active mass at the electrodes or electrolyte decomposition.

Definition of Aging in the Context of Batteries: The aging of batteries cannot be described by an absolute value. As described above the EOL of a battery has to be defined in the context of the application it is intended for. The most common definition for the end of life is a capacity loss of 20 % compared to the nominal capacity or a doubling of the internal resistance. As a measure for the state of aging the state of health (SOH) is often used. The state of health is defined to be one for a new battery and linearly decreasing to zero. A state of health of zero is reached at the EOL of the battery.

The aging behavior of batteries is typically differentiated between the float aging and the cyclic aging where the first describes the aging due to the progress in time and is mainly influenced by the temperature of the battery and the potential at which the battery is kept. It has been shown in [4], that the aging behavior of lithium-ion batteries is not only dependent on the ΔSOC and the battery temperature, but also shows a strong dependency on the absolute state of charge (SOC) or in fact the potential. Cycling the battery with identical cycle depth ΔSOC but at different cycling regimes (e.g. between 100 % SOC and 20 % SOC or between 80 % SOC and 0 % SOC) can lead to deviations in lifetime by a factor of 3 and more.

On the other hand the cyclic aging describes the loss of lifetime due to operation of the storage. On the cyclic aging the depth of the cycles ΔSOC has a main impact as the intercalation and deintercalation of ions into the electrodes causes a change in volume of the active material and therefore mechanical stress. The cyclic aging is typically defined by means of a Woehler diagram that correlates the number of performable cycles to the ΔSOC of the cycle. It gives the maximum number of cycles a cell can drive till the end of life, given the cycle depth. An example of such a Woehler diagram is shown in Figure 1. The Woehler diagram is usually given by the cell manufacturer. Also during cycling the effects of float aging take part.

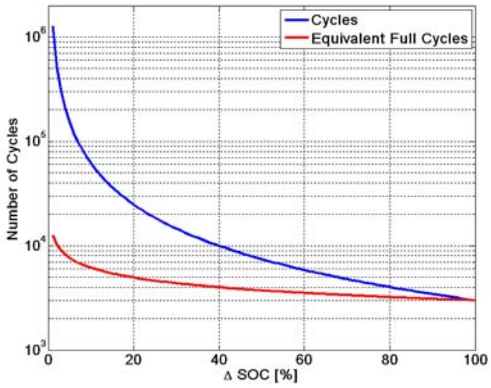

Figure 1: Woehler Curve

3 BATTERY MODEL

3.1 Model Approach

Based on an electric model of a lithium-ion battery, this paper focuses on an advanced aging model. The battery model used is based on an impedance driven approach. The electrical behavior is represented by the open circuit voltage (OCV) of the battery that has been measured at different temperature and state of charge levels and is passed to the model via a look-up table depending on the states of ambient temperature and SOC at a certain time step. Additional overvoltages are calculated via impedances according to the equivalent circuit depicted in Figure 2, dependent on the current applied to the battery.

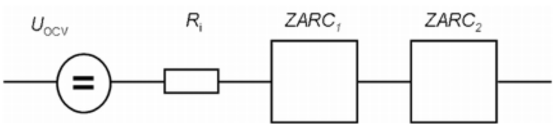

Figure 2: Equivalent Circuit of the Battery Model

The so called ZARC elements represent a parallel connection of a constant phase element and a resistance. It is a common representation for the semi-circles occurring in impedance spectra of batteries and can be modeled by a series connection of multiple parallel connected resistances and capacitors (RC elements) depending on the accuracy to be achieved. In the present model a series connection of 5 RC elements is used for each ZARC element. The impedance based modeling approach is well known and a detailed description is given in [1]

The impedance values have also been evaluated for different temperature and state of charge levels by means of impedance spectroscopy. Within certain bounds this model approach is suitable to represent the highly non-linear behavior of batteries. A good overview on the principle of electrochemical impedance spectroscopy is given in [2].

3.2 Model Assumptions

The parameters used are taken from measurements on a commercial lithium-ion battery of 7.2 Ah capacity.

4 AGING MODEL

The aging model presented in this paper focuses on the aging effects caused by the different impact factors described above. As input parameters the temperature and the SOC are passed to the model. The output of the model is an aging factor, representing the lifetime consumed during a certain period of time. The model does not account for the physico-chemical processes, therefore the aging mechanisms, taking place inside the battery. It is a heuristic approach that is intended to support system integrators to identify the optimum sizing and the optimum operation strategy in order to minimize the life cycle cost of their application based on a more or less simple parameterization of the battery and aging model. This model is not capable of making a statement about optimization of the internal battery design.

4.1 Consideration of Float Aging

The float aging model considers for the influence of the temperature and the state of charge on the aging. The impact of temperature on the battery aging is considered according to Arrhenius' law where an increase of temperature by 10 – 15 K halves the lifetime. The reference temperature T_0 for which the reference calendar lifetime $t_{\mathrm{cal,ref}}$ is obtained, the temperature difference ΔT leading to a bisection of lifetime and the battery temperature T_{bat} are passed to the model. and the resulting aging factor is then calculated according to

$$c_{\mathrm{temp}} = \frac{1}{t_{\mathrm{cal,ref}}} \cdot \int_{t_0}^{t_1} 2^{\left(\frac{T_{\mathrm{bat}} - T_0}{\Delta T}\right)} \mathrm{d}t$$

The impact of the state of charge is considered using an exponential function of the form

$$c_{\mathrm{SOC}} = \frac{1}{a + b \cdot \exp(c \cdot (100 - SOC))}$$

The parameters have been assumed to be

$$a = 2$$
$$b = -1.2$$
$$c = -0.0275$$

leading to a curve shown in Figure 3.

The SOC related term is multiplied by the temperature dependent term and the overall aging factor is calculated as follows:

$$c_{\mathrm{float}} = \frac{1}{t_{\mathrm{cal,ref}}} \cdot \int_{t_0}^{t_1} \frac{2^{\left(\frac{T_{\mathrm{bat}} - T_0}{\Delta T}\right)}}{a + b \cdot \exp(c \cdot (100 - SOC))} \mathrm{d}t$$

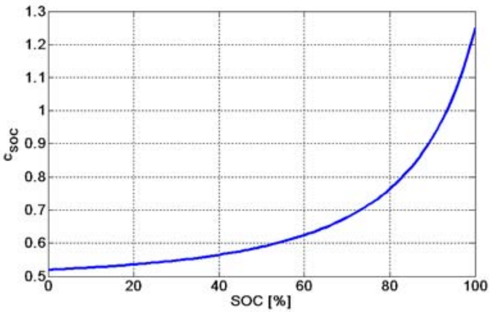

Figure 3: Dependency of the Aging Factor on SOC

4.2 Consideration of Cyclic Aging

As described above the cycle number and cycle depth influence the aging and degradation of lithium-ion batteries according to the Woehler diagram. For the calculations described in the following it is assumed that the Woehler characteristic corresponds to a potential function of the form

$$N_{\max,\Delta\mathrm{SOC}} = a \cdot \Delta SOC^{b},$$

where $N_{\max,\Delta\mathrm{SOC}}$ is the number of cycles that can be obtained given the cycle depth ΔSOC. The parameters a and b are recalculated from two pairs of corresponding values of the number of cycles $N_{\max,\Delta\mathrm{SOC}}$ and cycle depths ΔSOC.

As direct cycles often go along with long-term trends, a cycle counter was developed, that identifies micro cycles as well as longer charging or discharging phases. It is important to include macro cycles in the aging model, since a higher cycle depth increases the volume change in the battery and therefore the aging effect. Based on the number of cycles at given cycle depth, a cycle aging factor is calculated using a Woehler diagram.

The micro cycle profile is simply given by the actual charge profile of the battery as an array of time, SOC and Ah-throughput. Micro half-cycles are easy to detect using the change of sign of the applied current. They are stored in an array containing cycle depth, starting time and ending time. The detection of macro half-cycles is much more difficult. A smoothing of the charge profile by averaging has the disadvantage of cutting off the absolute extrema and therefore adulterates the aging results. A proceeding for the detection of macro half-cycles has been developed, based on the elimination of data points in the micro cycle profile. Therefore the micro cycle profile is divided into time intervals given by the user. For each interval an approximation straight through the maximum and minimum of the interval is constructed as well as a tolerance belt around the straight defined by the user. All data points inside the tolerance belt are deleted from the micro cycle profile except for the maximum, the minimum and the edge points of the interval. This leads to a smoothing of the original profile.

Going through the interval a macro cycle profile is generated and additionally smoothed to eliminate boundary effects. Macro half-cycles can now be easily detected in the macro cycle profile and stored in an array in the same way as the micro cycles. To prevent double counting, cycles occurring in the micro profile as well as in the macro profile have to be deleted from the macro half cycle array.

Figure 4 shows an example where the tolerance band (green lines) is chosen too wide. The resulting macro cycle profile (black line in the right graph) is identical to the micro cycle profile and does therefore have no effect on the aging factor. In Figure 5 the same profile is analysed with a smaller tolerance belt. All data points lie outside the tolerance belt and are therefore deleted. The resulting macro cycle is the black line having been constructed through the minimum and maximum value within the interval.

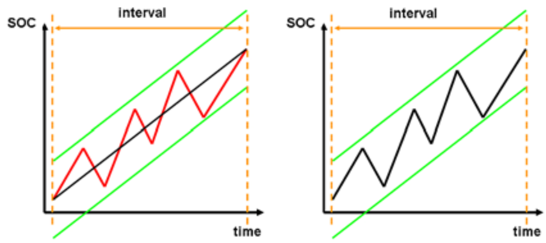

Figure 4: Wide Tolerance Belt - No Macro Cycle Effect

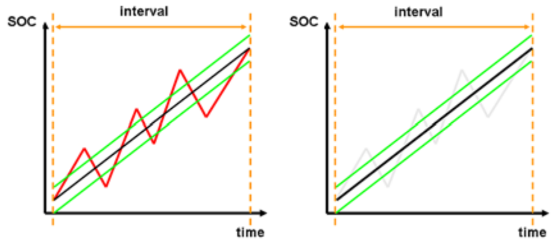

Figure 5: Small Tolerance Belt - Macro Cycle Detected

The two most important parameters the user passes to the model are the interval width for the division of the micro cycle profile and the width of the tolerance belt. The interval width should equal the time span in which a long-term drift usually takes place. The width of the tolerance belt should correspond to the depth of the cycle the user wants to filter out. Repeated runs with varying interval width and width of tolerance belt can be realised to detect macro cycles with different cycle depth.

After detecting the number of cycles for different cycle depths in the charge profile, the aging factor can be calculated based on a Woehler diagram. As the cycle detector only detects half-cycles, we have to assume, that the battery ages by the same amount during the charging and discharging process. Additionally we have to assume that,

- the aging of the battery is small during one cycle
- the aging during a cycle is independent of the previous events
- the aging during a cycle is independent of the age of the battery

The loss of lifetime of a cell can then be described by a factor

$$c_{\mathrm{cycle}} = \sum_{i} \frac{N_{\Delta\mathrm{SOC}}}{N_{\max,\Delta\mathrm{SOC}}},$$

where $N_{\Delta SOC}$ denotes the number of detected cycles at a given cycle depth ΔSOC and $N_{\max,\Delta SOC}$ the maximum number of cycles at cycle depth ΔSOC till the end of life. The aging factor including the micro cycles can be calculated easily using the equation above. In the aging factor due to macro cycles an Ah-correction factor has to be included, as the Ah-throughput following the macro cycle profile is lower than the actual Ah-throughput of the cell. The weighting factor is given by the following equation:

$$w = \frac{Q_{\text{macro}}}{Q_{\text{micro}}},$$

where Q_{macro} and Q_{micro} describe the charge throughput of the macro and the micro cycles respectively.

Finally, the aging factors of macro- and micro cycles are added up and passed to the output of the cycle aging block. The total cycling aging factor is calculated for a period of time corresponding to the previously defined interval width. It has to be assured that the effect of aging during the interval width is small as the charge profile is evaluated over the chosen interval width at once and its effect on the state variables, capacity and internal resistance, of the model is computed. The Woehler curve parameters applied to the model are based on the following assumptions:

$$\Delta SOC_1 = 100\,\%$$
$$N_{\max,100\%} = 3000$$
$$\Delta SOC_2 = 3\,\%$$
$$N_{\max,3\%} = 300000$$

The resulting parameters *a* and *b* are:

$$a = 1.2698 \cdot 10^6$$
$$\mathrm{b} = -1.3133$$

The Woehler diagram obtained by using those parameters corresponds to the curve shown in Figure 1.

4.3 Calculation of the Resulting Aging Factor

To calculate the resulting aging factor that determines the model behavior, it is assumed that different aging mechanisms are responsible for the float aging and the cyclic aging. As described above, the cyclic aging is mainly due to the mechanical stress induced by the volume change of the active material and therefore dependent on the ΔSOC within one cycle. On the other hand the float aging is driven by chemical degradation processes that are influenced by the temperature and the cell potential. The assumption made in this model is that one of the processes, either the float aging or the cyclic aging is dominating, depending on the operation conditions. Thus the resulting aging factor is calculated by taking the maximum value out of the two aging factors that are calculated in the different model components. The resulting aging factors that are calculated over a certain period of time, according to the interval width of the cyclic aging model, are then summed up over the simulation time in order to obtain the overall aging.

4.4 Aging behavior of the Battery

The sum of the resulting aging factors is passed to the battery model. For the aging behavior the simplified assumption is made that the capacity fade and the increase of the internal resistance are showing linear behavior over the lifetime and are taking place at the same time. The capacity C and the internal resistance R_{i} can therefore be calculated at a certain point in time using the following equation:

$$C(t) = C_{\text{nom}} \cdot (1 - 0.2 \cdot (1 - SOH(t_0) + c(t)))$$

$$R_{\mathrm{i}}(t) = R_{\text{nom}}(t_0) \cdot (1 + (1 - SOH(t_0) + c(t)))$$

where C_{nom} and R_{nom} are the nominal values of the capacity and the internal resistance, t_0 is the start time of the simulation, *SOH* is the state of health, and *c* is the aging factor. As the SOC is calculated on the actual capacity and the overvoltages are calculated by the resistance values this modification of the state variables allows for a closed loop calculation considering the performance loss of the battery over the lifetime.

5 SIMULATION ENVIRONMENT

In order to analyze the model behavior the battery model has been integrated into a time series based system model of a grid-connected PV system according to the Sol-ion approach. The scheme of the system is depicted in Figure 6, the red arrows showing the directions of possible energy flows.

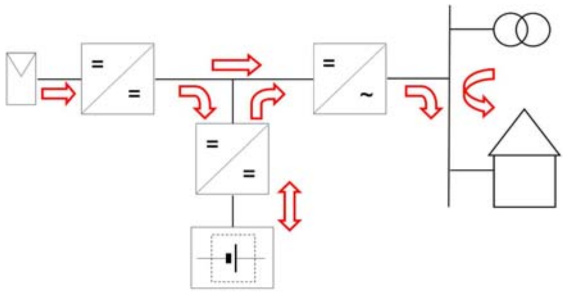

Figure 6: System Configuration

5.1 PV Generator

The PV generator is modeled based on the approach presented in [5], calculating the power and voltage output at the MPP, given the irradiation data in form of global, diffuse and beam irradiation and the temperature profile of the solar modules. The temperature is considered by means of the temperature coefficient, which is passed via an input parameter. This model can be parameterized using three pairs of corresponding voltage and irradiation values as well as two pairs of corresponding current and irradiation values from the characteristic of the PV module to be modeled. The values are mostly available in the datasheets of the manufacturer.

Irradiation data with a sample time of 15 minutes from the "SoDa" solar database for a location in Germany obtained in 2005 is used. Due to a lack of temperature data the temperature is assumed to be constant. The size of the PV-System is chosen to be 5 kWp resulting in an annual energy output of approximately 4250 kWh at the DC bus.

5.2 Load

The load is modeled by means of the VDEW standard load profiles also available in 15 min resolution accounting for the seasonal deviations of consumption as well as for the deviations of the different days of a week. The standard profile H0 for a residential household is scaled to an annual consumption of 4000 kWh.

5.3 Converter

The converters have been modeled using the model approach also described in [5]. This model can be easily parameterized using three pairs of values of the converter efficiency characteristic (either related to its input or its output power) and the nominal efficiency. In order to consider the voltage dependency, that especially has to be taken into account for the PV converter and the battery converter, it is possible to input multiple sets of parameters of efficiency curves, each related to a certain voltage. The resulting efficiency curve is then linearly interpolated from the given efficiency curves according to the input voltage. The converters have been parameterized by characteristics of commercial converters and have been scaled to a maximum power of 5 kW.

5.4 Energy Management

The maximum state of charge of the battery SOC_{max} can be set to an arbitrary value. Limiting the SOC_{max} to a value below 100 % will extend the lifetime as for the cyclic model the cycle depth ΔSOC is limited and for the float model the upper SOC values are not reached, which are more damaging to the battery.

The energy management is designed in a way that the complete load demand is satisfied by the PV generator as long as the generation is larger than the consumption. The surplus of generated power in this case is fed to the battery as long as the maximum allowed state of charge SOC_{max} is not exceeded. As soon as the SOC_{max} of the battery is reached the surplus is fed to the grid. If the PV generation stays below the load demand the lack of energy is taken from the battery as long as the SOC is greater than zero. Not until then the lack of energy is supplied by the grid. This energy management strategy accounts is intended to increase the self consumption of the PV energy according to the new incentive of the German renewable energy sources act (EEG) in its actual reading from January 2009.

5 SIMULATION

5.1 Simulation Scenarios

As this work focuses on the aging model the parameters for the battery as well as for the converters are chosen in order to point up the behavior of the aging model and are not representing the real system data of the components used in the Sol-ion project. In order to see the impact of the SOC dependency of the aging the temperature has been kept constant for all simulations and has been set to the reference value for the float lifetime that has been chosen to be 20 °C. The float lifetime has been assumed to be 15 a at 20 °C at a state of charge of 95 %. By variation of the battery size between 1 kWh and 10 kWh with steps of 1 kWh, and the maximum allowed state of charge SOC_{max} varied between 60 % and 100 % in steps of 20 % a full set of simulations has been performed.

For a PV battery system the macro cycles are expected to occur in daily intervals caused by the daily cycle of the sun. The battery is charged during daytime and discharged during the night. Based on this fact the interval width for the aging factor calculation is set to be one day.

6 SIMULATION RESULTS

Figure 7 shows the obtainable lifetime depending on the size of the battery for the different SOC_{max} values.

It can be seen that for small batteries the aging is dominated by the cyclic aging thus leading to lifetimes well below the reference float lifetime of 15 years for the 100 % and 80 % scenarios and slightly above for the 60 % scenario. For a small battery it can be assumed that the battery is charged and discharged over the total allowed ΔSOC range during one day and night cycle even during winter days.

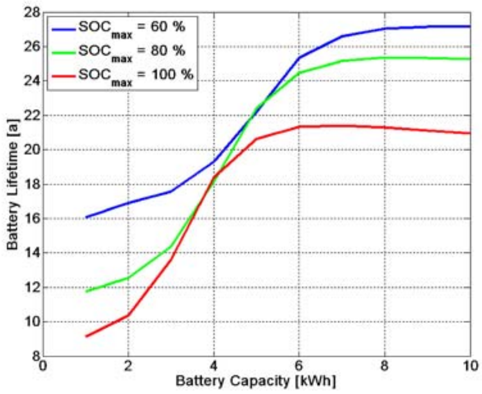

Figure 7: Lifetime Depending on Battery Capacity

For the battery not being limited regarding the SOC_{max} this means one full cycle where the batteries limited to 80 % and 60 % perform one 80 % or one 60 % cycle per day respectively. It can be seen that the lifetime approaches a saturation value for all three curves. These values can be estimated using the Woehler curve by

$$L = \frac{N_{\max,\Delta SOC}}{N_{a,\Delta SOC}},$$

where $N_{max,\Delta SOC}$ is the maximum number of cycles performed with a given cycle depth ΔSOC and $N_{a,\Delta SOC}$ is the number of cycles per year with the same cycle depth. According to the assumptions given above $N_{a, \Delta SOC}$ is 365 for all the three cases and $N_{max,\Delta SOC}$ is 100 %, 80 % or 60 % respectively.

Moving along the curves towards larger battery sizes, leads to an increase in lifetime. This can be explained by the fact that with increasing battery size the cycles become shallower especially during winter days where the PV generation is low. According to the Woehler curve shallower cycles lead to decreased cyclic aging. So moving towards larger capacities continuously increases the impact of the float aging and in the end leads to lifetimes limited by the float aging. As the reference float lifetime is assumed to be given for a battery at 95 % SOC the resulting float lifetime is longer than the assumed reference lifetime of 15 years.

It can be seen that the steepness of the fading from cyclic to float aging is increasing with increasing SOC_{max}. Because of the limitation of the SOC_{max} to lower values the increase in usable capacity is lower compared to the case where the SOC_{max} is not limited. The increase of battery has to be scaled by SOC_{max} in order to obtain the increase in usable capacity. So for the case where SOC_{max} is 100 % the increase of the battery capacity leads to an increase of usable capacity of the same amount, whereas the increase of battery capacity is scaled with 80 % or 60 % for the other curves respectively. This in fact causes the effect of the cycles becoming shallower by increase of battery capacity to be amplified for larger SOC_{max} values and thus causes the steeper increase of lifetime.

Finally the lifetime curve of the case with 100 % SOC_{max} shows a maximum, decreasing again when moving to even larger capacity values. Also this can be explained having a look at the SOC profile over one year obtained for a large capacity and a SOC_{max} of 100 %, as shown in Figure 8.

During summer days the daily load demand is less than the daily PV generation. Increasing the battery size above the daily load demand thus causes the battery to be fully charged within a few sunny days but to be not fully discharged during night.

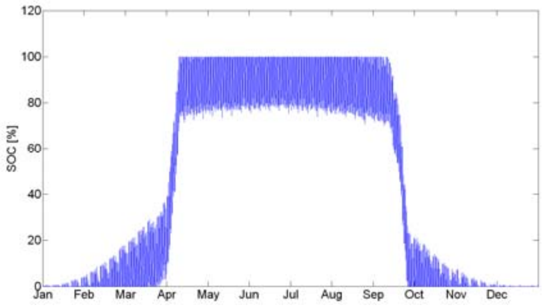

Figure 8: SOC Profile over 1 Year - 10 kWh Battery

By increasing the capacity far above the daily load demand therefore keeps the battery in the upper SOC range for quite a long period and any further increase just limits the SOC range to even higher values as the cycle depth with respect to the battery capacity decreases. Due to this the battery lifetime decreases again.

Talking about life cycle costs (LCC) an increased battery lifetime does not imply reduced LCC. In order to compare the costs of the different simulation scenarios Figure 9 shows the battery investment cost related to the additional energy that can be locally consumed through the installation of the battery.

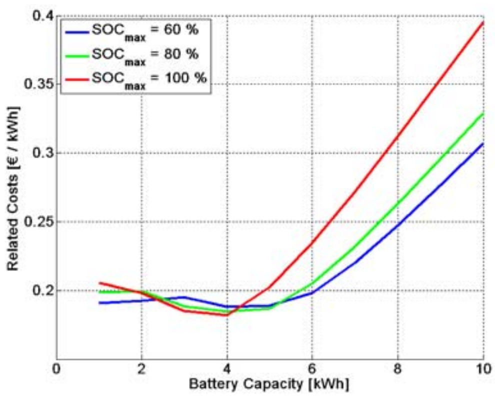

Figure 9: Related Battery Costs

The related costs are calculated according to:

$$LCC_{\text{simple}} = \frac{W_{\text{nom,E}}\,[\text{kWh}] \cdot 1000\text{ €}}{L\,[\text{a}] \cdot E_{\text{bat}}\,[\text{kWh/a}]},$$

where $W_{\text{nom,E}}$ is the nominal energy capacity of the battery, L is the lifetime according to Figure 7 and E_{bat} is the additional energy that can be locally consumed through installation of the battery. The investment cost for the battery of 1000 € / kWh is an arbitrary chosen value that reflects a realistic value at the instant. It can be seen that all curves show local minima in the range of 4 to 5 kWh installed battery capacity. The increase of battery capacity gathers only slightly increasing benefit from a certain point, as can be also seen from Figure 8. As soon as the battery becomes much larger than the average daily load demand, the battery is only driven to higher levels during summer and therefore the additional obtainable energy is only that of the slopes in spring and autumn becoming longer.

Although the obtained lifetime with SOC_{max} = 100 % is the lowest over nearly the full range the absolute minimum of cost can be found for this operation condition.

The presented cost calculation is a simplified way of relating the investment to the benefit. The costs per kWh shown in the graph cannot be taken as absolute values as this simple approach does not replace a full life cycle cost assessment. Nevertheless it makes clear that the maximization of the lifetime can not be the measure to design the battery management system or the battery size.

7 CONCLUSION

The model presented is capable of considering the different operation conditions causing aging to appear. The simulated influence of different impact factors shows a good agreement with the expectancy. Although the simulations are still based on assumptions, the model shows up the importance of considering all the impact factors.

As the model is based on a heuristic approach still a lot of parameters have to be set. The parameters to properly represent a given battery have to be obtained by extensive measurements. As a system integrator will not be able to perform all those measurements for a battery, let alone for various batteries, in order to make a choice for his application, in the long term sufficient data has to be provided by the battery manufacturers.

In a next step of modeling, assumptions have to be replaced by significant data. The following assumptions have therefore to be checked:

- the temperature dependency can be described properly by Arrhenius' law, also under cycle operation
- the dependency of aging on the SOC / voltage follows an exponential function
- the cyclic aging described by the Woehler curve follows a potential function
- the relation between macro and micro cycle induced aging can be weighted by the charge throughput

8 ACKNOWLEDGEMENT

The presented paper is partly based on results of the project 'Netzgekoppelte PV-Systeme mit Lithium-Ionen Speichern zur Verbesserung der Integration von Erneuerbaren Energien in das öffentliche Stromnetz (Sol-ion)', supported by the German Federal Ministry for the Environment, Nature Conservation and Nuclear Safety

(BMU). The authors take full and sole responsibility for the content of this paper.

9 REFERENCES

[1] S. Buller, *Impedance-Based Simulation Models for Energy Storage Devices in Advanced Automotive Power Systems*, Aachener Beiträge des ISEA, Vol. 31, Shaker Verlag, February 2003

[2] E. Karden, *Using low-frequency impedance spectroscopy for characterization, monitoring, and modeling of industrial batteries,* Dissertation, ISEA, RWTH Aachen University, February 2001

[3] J. Vetter, P. Novak, M.R. Wagner, C. Veit, K.-C. Möller, J.O. Besenhard, M. Winter, M. Wohlfahrt-Mehrens, C. Vogler, A. Hammouche, J. Power Sources 147 (2005) 269-281

[4] Takei, K.; Kumai, K.; Kobayashi, Y.; Miyashiro, H.; Terada, N.; Iwahori, T.; Tanaka, T., J. Power Sources 97 – 98 (2001) 697 - 701, 2001

[5] D.U. Sauer, Untersuchungen zum Einsatz und Entwicklung von Simulationsmodellen für die Auslegung von Photovoltaik-Systemen, Diploma Thesis, Technische Hochschule Darmstadt, April 1994